DOI: http://dx.doi.org/10.22104/aet.2016.361

Advances in Environmental Technology 1 (2016) 33-44

Advances in Environmental Technology

journal homepage: http://aet.irost.ir

Response surface methodology and artificial neural network modeling of reactive red 33 decolorization by O_3/UV in a bubble column reactor

Jamshid Behin[*], **Negin Farhadian**

Department of Chemical Engineering, Faculty of Engineering, Razi University, Kermanshah, Iran

ARTICLE INFO

Article history:
Received 22 April 2016
Received in revised form
7 September 2016
Accepted 3 October 2016

Keywords:
Artificial neural network
Bubble column
Ozone/Ultraviolet
Response surface method
Reactive red 33

ABSTRACT

In this work, response surface methodology (RSM) and artificial neural network (ANN) were used to predict the decolorization efficiency of Reactive Red 33 (RR 33) by applying the O_3/UV process in a bubble column reactor. The effects of four independent variables including time (20-60 min), superficial gas velocity (0.06-0.18 cm/s), initial concentration of dye (50-150 ppm), and pH (3-11) were investigated using a 3-level 4-factor central composite experimental design. This design was utilized to train a feed-forward multilayered perceptron artificial neural network with a back-propagation algorithm. A comparison between the models' results and experimental data gave high correlation coefficients and showed that the two models were able to predict Reactive Red 33 removal by employing the O_3/UV process. Considering the results of the yield of dye removal and the response surface-generated model, the optimum conditions for dye removal were found to be a retention time of 59.87 min, a superficial gas velocity of 0.18 cm/s, an initial concentration of 96.33 ppm, and a pH of 7.99.

1. Introduction

Large amounts of chemicals (more than 10000 dyes) are used in the textile industry during the finishing and dying processes [1]. Azo dyes are environmentally hazardous materials due to their toxicity and slow degradation [2-4]. The treatment of azo dyes effluents to meet the stringent environmental regulations is necessary prior to their final discharge into the environment [5-7]. Different conventional methods consisting of various combinations of biological, physical and chemical methods have been used in order to deal with textile wastewater, but these methods are not as efficient as advanced oxidation processes (AOPs) [8-10]. AOPs are chemical methods based on the generation of high reactive hydroxyl radicals ($OH^{\cdot}$) that can oxidize the contaminants powerfully and non-selectively. A number of AOPs such as ozonation (O_3), hydrogen peroxide (H_2O_2), O_3/UV, O_3/H_2O_2, $O_3/UV/H_2O_2$, UV/TiO_2, UV/ZnO and recently O_3/Ultrasound (US) have been well studied [11-15]. The combination of O_3 with UV, which yields hydroxyl, peroxyl, and superoxide radicals, should synergistically accelerate the removal of organic matter from complex wastewater matrices [16]. As illustrated by Beltran [17] and Lucasa et al. [16], the O_3/UV process was capable of oxidizing wastewater faster than O_3 alone, showing a photochemical enhancement oxidation effect. This was principally due to the photolysis of ozone, the enhanced mass transfer of ozone, and the generation of hydroxyl radicals that reacted rapidly with the organic matter in the winery wastewater. Khan et al. [18] showed that the effectiveness of ozonation was enhanced by applying UV. Consequently, the reactant molecules were raised to a higher energy state and reacted more rapidly. Moreover, free radicals for use in the reaction were readily hydrolyzed by water. Another benefit of the combined use of ozone and UV was a substantial reduction in the amount of ozone required as compared to a system using O_3 alone [18]. Several literatures also reported that by combining UV irradiation with O_3, the oxidation power of the systems for

*Corresponding author. Tel.: +98-833-8250167
Fax: +98-833-8250167; E-mail: Behin@razi.ac.ir

organic pollutant degradation could be significantly enhanced [19-24]. Response surface methodology (RSM) has been widely used in process and product improvement. It is efficiently used to examine and optimize the operational variables for experiment designing and model developing [25, 26]. RSM is typically used for mapping a response surface over a particular region of interest, optimizing the responses, and selecting operating conditions to achieve target specifications or consumer requirements [27]. The decolorization of reactive blue 19 dye by Phanerochaete chrysosporium in an aqueous solution was optimized using the Box-Behnken design based on RSM [28]. Based on the central composite design (CCD), the optimization of the UV/TiO_2 process in the photo-reactor was carried out using RSM to assess the effects of the main independent parameters on the decolorization efficiency of the azo dye C.I. Basic Red 46 [29]. More recently, artificial neural networks (ANN) are increasingly used as predictive tools in an extensive range of disciplines, such as engineering, due to their ability to employ learning algorithms and discern input–output relationships for complex, nonlinear systems [30-32]. Some literature surveys have shown the application of AANs in water treatment that included the removal of acid orange 7 by activated carbon [33], basic Red 46 degradation using photoelectro-fenton combined with the photocatalytic process [34], and the removal of four different dyes from an aqueous medium by a peroxi-coagulation method using a carbon nanotube (CNT) cathode [35]. Nowadays, RSM and ANN approaches are applied for optimization and process modeling [36-41]. A comparison of the predictive and generalization capabilities, sensitivity analysis, and optimization abilities of ANN and RSM techniques revealed that the ANN model fit the data better and had a higher predictive capability than RSM, even with the limited number of experiments.

Sinha *et al*. [41] used RSM and ANN modeling of microwave assisted natural dye extraction from pomegranate rind to optimize the effects of processing parameters and to get a good correlation between the input variables and the output parameter. Maran et al. [42] performed a comparative study between ANN and RSM to predict the mass transfer parameters of the osmotic dehydration of papaya. The results showed that the ANN model was more accurate in prediction as compared to the RSM model. The decolorization process of the dye was carried out by bubbling O_3 in a bubble column reactor containing the dye solution. The gas flow ensured both the O_3 (oxidant) supply and the efficient mixing (high mass transfer of ozone) without the need for mechanical mixing. The experiments were conducted using a batch bubble column to take advantage of the intensive back-mixing that prevailed in the bubble columns. The strong back-mixing reduced the mixing time between the reactants and accelerated the process of decolorization. In addition, the bubble columns were simple in their design and operated in the absence of mechanical moving parts. A reactor that provided the benefits of high efficiency, low energy input, and easy construction to improve decolorization efficiency was necessary. Decolorization in the bubble column photo-reactor had many advantages such as convenience, economy, safety and high efficiency and as a consequence, it can be considered a good prospect in future applications. The main motivation behind this study was the utilization the RSM and ANN methodologies for predicting the decolorization of Reactive Red 33 (RR 33) by the O_3/UV process; the results obtained through RSM were then compared with those obtained through ANN. A number of experiments were carried out based on CCD to collect the output variable (decolorization efficiency) as a function of time, superficial gas velocity, initial concentration of dye, and pH. A feed-forward neural network on back-propagation were developed utilizing the experimental data.

2. Materials and methods

Reactive Red 33 ($C_{27}H_{19}ClN_7Na_3O_{11}S_3$) was taken from the Boyakhsaz Company, Iran. The experimental setup consisted of a laboratory scale bubble column reactor that was 6.5 cm in diameter and 50 cm in height which was placed inside a photochemical chamber that contained four UV_{AB} lamps (Narva, Germany) of 15 W. Each lamp was placed in a 90° angle to another. The diameter and length of each lamp was 2.5 mm and 45 cm, respectively. Figure 1 shows a schematic of the set-up used for the experimental runs. The reactor was filled with 1 L of aqueous dye solution. An ozone-air mixture was continuously bubbled into the solution throughout a gas distributer that was placed at the bottom of the reactor. Ozone was generated in an ozone generator (Arda, France). The gas flow rate was monitored with a calibrated rotameter incorporated in the ozone generator. The ozone concentration was measured by the iodometry method (KI solution). Liquid samples of 5 mL were withdrawn by a pipette at specific intervals and then analyzed for dye concentration. The dye concentration was determined using a 2100-UV Spectrophotometer (Unico, USA) with a maximum absorption wavelength of 509 nm. The pH of the liquid solution was adjusted using H_2SO_4 (1 N) or NaOH (1 N). All experiments were carried out at a constant temperature of 25±2°C. The dye decolorization efficiency (Y) was calculated by the following equation:

$$\mathrm{Y}\,(\%) = 1 - \frac{C_A}{C_{A_o}} \tag{1}$$

Where C_A is the concentration of dye (ppm) and C_{Ao} is the initial concentration of dye (ppm).

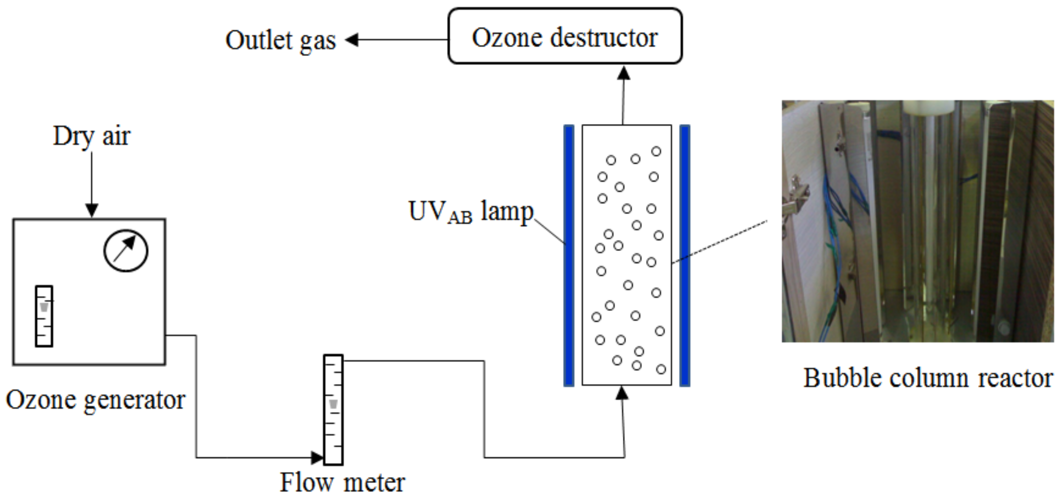

Fig. 1. Experimental set-up and bubble column reactor

2.1. Experimental design

RSM was applied to the experimental data using statistical software, namely Design-expert V7 (trial version). Central composite design (CCD) in RSM was used to develop a response surface quadratic model for describing the dye decolorization process. The ranges and levels of variables investigated in the research including time, superficial gas velocity, initial dye concentration, and pH are given in Table 1. Data from CCD were subjected to the following quadratic equation model to predict the system response and estimate the coefficients by the least-squares regression:

$$Y = \beta_0 + \sum_{i=1}^{k} \beta_i X_i + \sum_{i=1}^{k} \beta_{ii} X_i^2 + \sum_{i=1}^{k-1} \sum_{j=2}^{k} \beta_{ij} X_i X_j + e \quad (2)$$

Where Y is the predicted decolorization efficiency of RR 33; β_o is the model intercept coefficient; β_i, β_{ii} and β_{ij} are respectively the linear, quadratic and interaction coefficients; X_i and X_j are the independent variables; and e is the error. The statistical significance of each regression coefficient on the decolorization of RR33 was determined by analysis of variance (ANOVA).

Table 1. Experimental variables and levels

Variable	Symbol	Unit	Low	Middle	High
			-1	0	1
Time	A	min	20	40	60
Superficial gas velocity	B	cm/s	0.06	0.12	0.18
Initial dye concentration	C	ppm	50	100	150
pH	D	-	3.0	7.0	11.0

2.2. Artificial neural networks

The Back Propagation Algorithm (BPA) was applied to train the neural network. The BPA modified network weights to minimize the MSE between the desired and the actual outputs of the network. A feed forward back propagation neural network with three layers was used. The layers of network contained an input layer, hidden layer and output layer. In the feed forward neural network, information flowed from input to output without feedback [43]. It had one hidden layer with a sigmoid transfer function followed by an output layer with a linear transfer function. Multiple layers of neurons with nonlinear transfer functions allowed the network to learn nonlinear and linear relationships between input and output vectors [44]. It has been reported that multilayer ANN models with only one hidden layer have universal applications [45]. The neural networks toolbox of Matlab 7.12.0 was used. Figure 2 illustrates ANN (4:n:1) for the modeling of the UV/O_3 degradation process in which n is the number of neurons in the hidden layer.

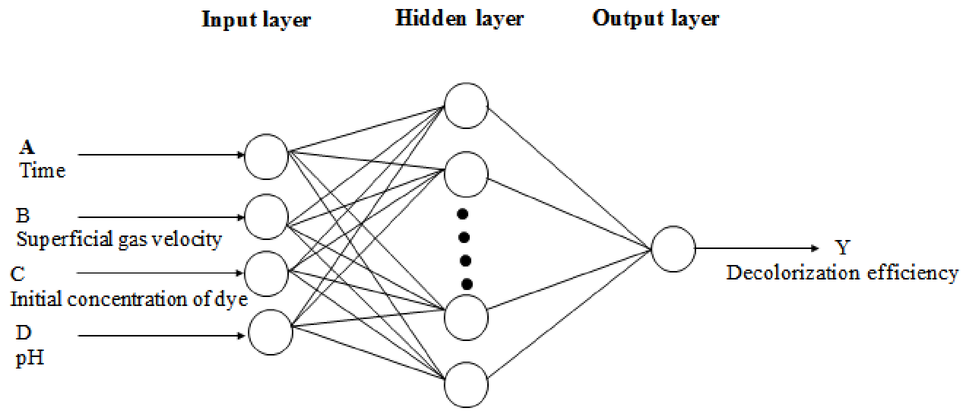

Fig. 2. Conceptual structure of 3 layer ANN model

3. Results and discussion

3.1. RSM modeling

According to the CCD, the experiments were performed in order to determine the optimum combination and study the effect of process variables on the decolorization efficiency of RR33. Table 2 depicts the four-factor, three-level CCD and the observed values for the RR33 decolorization efficiency by the developed quadratic model. The empirical relationships between the response and the four independent variables have been expressed in terms of unit less regression coefficient by the quadratic model and are given as:

$$Y = 90.76 + 13.11\,A - 4.92\,B - 7.76\,C + 3.78\,D + 5.35\,A.\;B + 6.63\,A.C - 3.01\,A.\;D - 0.45\,B.C + 3.26\,B.C - 0.29\,C.D - 5.64\,A^2 - 1.47\,B^2 - 2.20\,C^2 - 0.84\,D^2 \quad (3)$$

Without considering the sign of regression model coefficients for variables and interactions, the order of effectiveness of all variables and their binary interactions is as follows (higher model coefficient in absolute values):

$A > C > AC > A^2 > AB > B > D > BC > AD > C^2 > B^2 > D^2 > BC > CD$

Table 3 shows the results of the second-order response surface in the form of analysis of variance (ANOVA); the results indicated that the equation adequately represented the actual relationship between the independent variables and the responses. The positive or negative sign of model coefficient values described the direction of each variable or interaction effect on the response, i.e., positive values variables' increment caused increases in decolorization yields while negative values variables' increment caused a decrease in decolorization yield. Table 3 shows that the two main factors (A, D) and the three binary interaction effects (AB, AC, BC) had positive signs; all other effects (B, C, AD, BC, CD, A^2, B^2, C^2, D^2) had negative signs and a reverse effects on the responses. The ANOVA results (Table 3) for the O_3/UV oxidation system shows the F-value to be 39.93, which implies that the terms in the model have a significant effect on the response. The linear terms were the four independent variables, which included A: time, B: superficial gas velocity, C: initial concentration of dye and D: pH with the largest effect on the response ($p < 0.0001$). The results suggested that the change of time, superficial gas velocity, initial concentration of dye, and pH had very significant effects on the efficiency of RR33 ($p < 0.0001$) when O_3/UV was used in the decolorization of dye. The model's terms with a probability value larger than 0.05 were not significant. The non-significant value of lack of fit (more than 0.05) showed that the quadratic model was valid for the present study. The goodness of fit of the model was examined by the determination of coefficient (R^2= 0.9739), which implied that the sample variation was 97.39% statistically significant and only 0.03% of the total variance could not be explained by the model. The regression model coefficient value, e. g. 13.11, for the retention time (A) was the most significant value in comparison with other variables. Obviously, an increase in the time of the decolorization process can result in a higher decolorization yield. According to the statistical results, the retention time increased the comparable changes in the decolorization yield of RR33 more than the other process variables. The positive sign of the model coefficient for retention time indicated the proportional effect of this variable on the decolorization yield, i.e., increasing retention time will increase the response. The amount of the *p*-value for the retention time was less than 0.05 for a 95% confident level. In order to analyze the regression equation of the model, three-dimensional (3D) surface and 2D contour plots were obtained by plotting the response (decolorization efficiency) on the Z axis against any two variables while keeping the other variable at middle level. These plots were created to analyze the change in the response surface. The surface and contour plots of the quadratic model are shown in Figure 3 (a-f). The plots were approximately symmetrical in shape; the nonlinear nature of all 3D response surfaces showed considerable interactions between the independent variables and the RR33 decolorization as a response function.

Table 2. Coded central composite design of independent variables and their corresponding experimental values

Run order	A	B	C	D	Decolorization efficiency (Y)
1	1	0	0	0	95.80
2	0	1	0	0	85.70
3	1	1	-1	-1	95.38
4	0	0	0	-1	85.20
5	0	0	0	0	86.40
6	-1	-1	-1	1	94.10
7	-1	-1	-1	-1	91.69
8	1	-1	-1	-1	93.24
9	-1	1	1	1	55.10
10	-1	1	-1	-1	57.80
11	1	-1	1	-1	94.20
12	0	0	1	0	80.88
13	-1	-1	1	-1	62.42
14	1	-1	1	1	93.80
15	0	0	0	0	92.60
16	0	-1	0	0	91.34
17	0	0	0	0	92.40
18	1	-1	-1	1	94.20
19	0	0	0	0	93.10
20	-1	1	-1	1	84.00
21	0	0	0	0	91.20
22	1	1	1	1	92.90
23	0	0	0	1	93.10
24	1	1	-1	1	98.20
25	-1	0	0	0	72.90
26	0	0	0	0	93.50
27	1	1	1	-1	90.29
28	0	0	-1	0	94.70
29	-1	-1	1	1	63.50
30	-1	1	1	-1	30.60

Table 3. Analysis of variance (ANOVA) for RR 33 decolorization efficiency (%)

Parameters	Statistics				
	Sum of squres	Degree of freedom	Mean square	F-value	P-value
Model	6962.11	14	497.29	39.93	< 0.0001
A: time	3091.60	1	3091.60	248.23	< 0.0001
B: superficial gas velocity	435.32	1	435.32	34.95	< 0.0001
C: initial concentration of dye	1082.99	1	1082.99	86.95	< 0.0001
D:pH	257.49	1	257.49	20.67	0.0004
AB	457.32	1	457.32	36.72	< 0.0001
AC	704.11	1	704.11	56.53	< 0.0001
AD	145.20	1	145.20	11.66	0.0038
BC	3.22	1	3.22	0.26	0.6184
BD	169.52	1	169.52	13.61	0.0022
CD	1.32	1	1.32	0.11	0.7490
A^2	82.37	1	82.37	6.61	0.0213
B^2	5.59	1	5.59	0.45	0.5132
C^2	12.52	1	12.52	1.01	0.3319
D^2	1.82	1	1.82	0.15	0.7075
Residuals	186.82	15	12.45		
Lack of fit	152.15	10	15.21	2.19	0.1996
Pure error	34.67	5	6.93		
Total	7148.93	29			
R^2: 0.9739					
Adjusted R^2: 0.9495					
Adeqate Precision: 27.004					
C.V. % : 4.17					
Pred R-Squared: 0.8289					

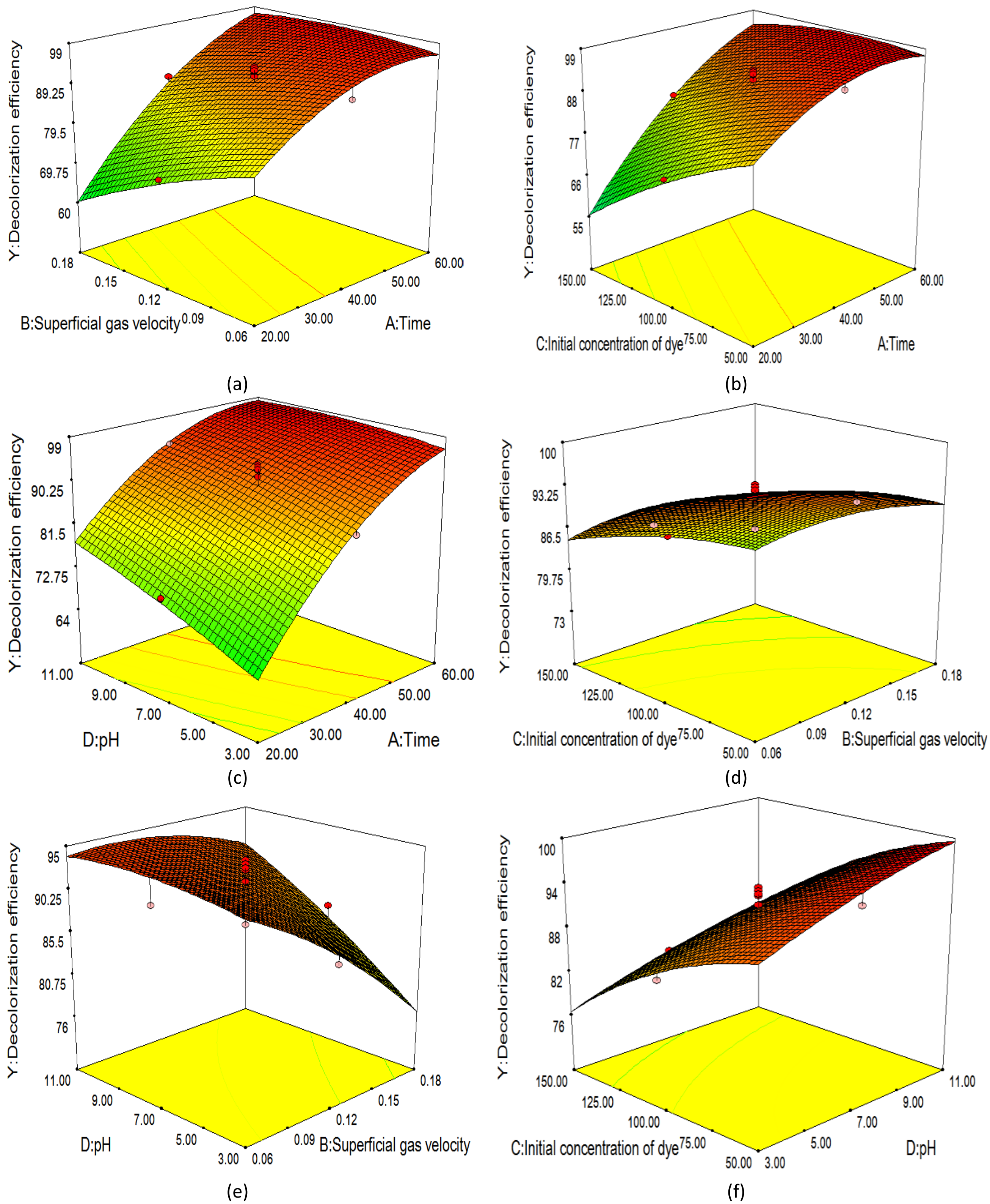

Fig. 3. Response surface plots showing the effect of independent variables on decolorization of RR 33

The AOP with UV irradiation and ozone was initiated by the photolysis of the ozone. The photo-decomposition of the ozone led to the formation of H_2O_2 in the following reaction:

$$O_3 + H_2O + h\nu \rightarrow H_2O_2 + O_2 \tag{4}$$

Consequently, the generation of two hydroxyl radicals occurred as a result of the following reaction:

$$H_2O_2 + h\nu \rightarrow 2OH^{\circ} \tag{5}$$

This system contained three components to produce OH radicals and/or oxidize the pollutant for subsequent reactions: UV irradiation, ozone and hydrogen peroxide [46]. All degradation mechanisms should be taken into consideration: OH radical attack as predominant, direct ozone attack, direct photolysis of organics by UV irradiation, and direct oxidation by H_2O_2 [47].

Figure 3 (c, e and f) represents the influence of pH on the color removal efficiency of ozone. There was an increase in the removal efficiency with an increase in the pH of the dye solution [48-50]. Higher color removal efficiency at a pH of 11 can best be explained by the fact that in a highly alkaline medium, the ozone dissociated to the hydroperoxide anions. The HO·radical was especially important in the decolorization process because of its high oxidation potential of 2.8 eV [51, 52]. The free radicals cleaved the conjugated bonds of the dye, resulting in decolorization. The pH tolerance was quite important because the reactive azo dyes bind to cotton fibers by the addition or substitution mechanisms under alkaline conditions and high temperatures [53, 54]. An increase in time enhanced the mass transfer, which resulted in increased ozone content in the liquid phase and an enhanced degradation rate constant [55]. Higher decolorization was achieved at low concentrations of RR33, as is shown in Figure 2 (b, d and f). It can be found that as the dye concentration increased, the decolorization rate constant decreased. Several studies have reported similar observations. The dye had a UV-screening effect and hence a significant quantity of UV light may be absorbed by the high concentration of dye molecules which reduced decolorization efficiency. Moreover, there are more dyes and reaction intermediates that competed with the OH radicals in the high initial concentration

[3, 56].From Figure 3(a, d, and e), it can be seen that the decolorization yield increased with the increase of superficial gas velocity. The increase in flow rate corresponded to a larger net surface area for the mass transfer of the ozone from the gas phase to the aqueous phase, and hence increased the volumetric mass transfer coefficient of the ozone. The concentration of the hydroxyl radicals increased with an increase in the ozone concentration. This resulted in a higher dye removal rate [57]. The optimum condition for the removal of RR33 was determined in order to obtain the maximum decolorization efficiency. In order to obtain maximum desirability, the decolorization efficiency was maximized while the independent variables were within range. The optimum condition was found to be a time of 59.87 min, a superficial gas velocity of 0.18 cm/s, an initial concentration of 96.33 ppm, and a pH of 7.99, respectively, with an overall desirability value of 1. The decolorization efficiency of the dye under these optimum conditions was found to be 98.19 and the experimental value was 99.10; the deviation of the experimental and theoretical results was found to be 0.92%. This indicated the suitability of the developed model.

3.2. ANN modeling

ANN methodology was performed to provide a nonlinear mapping between the input variables (time, superficial gas velocity, initial dye concentration and pH) and the output variable (decolorization efficiency) for the runs reported in Table 4. In order to increase the convergence speed and minimize the errors, the experimental data were normalized at {0 1} using a min-max formula:

$$x_n = (x_i - x_{min})/x_{max} - x_{min} \qquad (6)$$

Where x_n, x_i, x_{min} and x_{max} are normalized, real, minimum, and maximum value, respectively. The deviations used for selecting the best ANN architecture were the mean square errors (MSE) and the absolute fraction of variance (R^2) which can be defined as follows [58, 59]:

$$MSE = \frac{1}{N}\sum_{i=1}^{N}(t_i - y_i)^2 \qquad (7)$$

$$R^2 = \frac{\sum_{i=1}^{N}(t_i - t_m{}^2 - \sum_{i=1}^{N}(t_i - y_i)^2)}{\sum_{i=1}^{N}(t_i - y_i)^2} \qquad (8)$$

Where N is the number of data points, t is the target (experimental) data, and y is the predicted value. The back propagation algorithm was applied for the network training as the most suitable algorithm. In order to determine the optimum number of neurons in the hidden layer, a series of topologies was examined. The different number of neurons in the range of 1-15 was tested in the hidden layer. According to Table 4, the network with 6 neurons in hidden layer had the best results of MSE (2.89×10^{-5}) and R for both the training and testing data. As a result, in this study a three layered feed forward back propagation neural network (4:6:1) was used for the modeling of the decolorization process. The actual and predicted values by RSM and ANN are presented in Figure 4. The values of R^2 for the ANN and RSM models were found to be 0.9739 and 0.9989, respectively. The ANN model was able to capture the nonlinearities of the experimental data better than the RSM model with a combined regression coefficient of 0.998 for RR33 decolorization efficiency.

Table 4. Detail results of the various investigated neural networks structure

Model Structure	Training		Testing	
	MSE	R	MSE	R
4:1:1	6.31×10^{-3}	0.9718	1.45×10^{-2}	0.9567
4:2:1	3.47×10^{-3}	0.9757	2.54×10^{-3}	0.9341
4:3:1	1.07×10^{-4}	0.9976	4.33×10^{-2}	0.9743
4:4:1	5.06×10^{-4}	0.9959	4.85×10^{-3}	0.9711
4:5:1	1.00×10^{-4}	0.9990	1.34×10^{-3}	0.9384
4:6:1	2.89×10^{-5}	0.9996	7.46×10^{-3}	0.9989
4:7:1	1.78×10^{-3}	0.9851	3.85×10^{-3}	0.9875
4:8:1	5.28×10^{-4}	0.9960	3.09×10^{-3}	0.9640
4:9:1	1.88×10^{-4}	0.9986	2.36×10^{-2}	0.9789
4:10:1	3.79×10^{-4}	0.9969	5.63×10^{-3}	0.9290
4:11:1	2.89×10^{-3}	0.9920	1.34×10^{-2}	0.9726
4:12:1	2.28×10^{-4}	0.9955	7.62×10^{-2}	0.8257
4-13:1	9.69×10^{-4}	0.9885	8.41×10^{-2}	0.9720
4:14:1	3.28×10^{-4}	0.9947	2.24×10^{-2}	0.9573
4:15:1	7.28×10^{-4}	0.9957	5.57×10^{-2}	0.9533

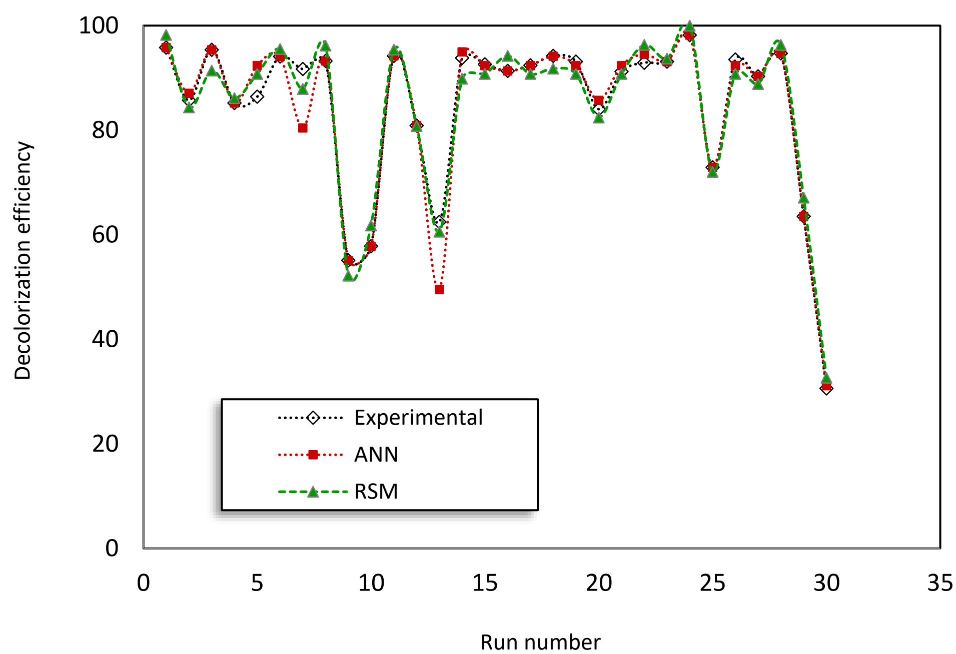

Fig. 4. Plot of the experimental and theoretical results of the RSM and ANN models

3.3. Decolorization kinetics

Several investigators [60-62] have reported that the decolorization process mainly follows first-order kinetics. The kinetics experiments were conducted under optimized reaction conditions for applied AOP. In the experiments, the disappearance of dye was described as first-order reaction kinetics with regard to the dye concentration. The corresponding first-order correlation is shown in Figure 5 which is the typical plot of linear regression (ln C_o/C_t) verses time for color removal. It can be observed that the correlation between in C_o/C_t and the irradiation time was linear. This was a typical pseudo first-order reaction plot. The kinetic expression can be presented as follows:

$$\ln\frac{C_t}{C_0} = -k.t \quad (9)$$

Where C_t is the dye concentration at instant t (ppm), C_o is the initial dye concentration (ppm), k is the pseudo first-order rate constant (min^{-1}), and t is the reaction time (min). The correlation coefficient that can explain the fitting extent of the function equation and the experimental data is presented by R^2. In this case, the value of R^2 is greater than 0.9, which confirms the accuracy of the assumed kinetics for the O_3/UV decolorization reactions of RR33.

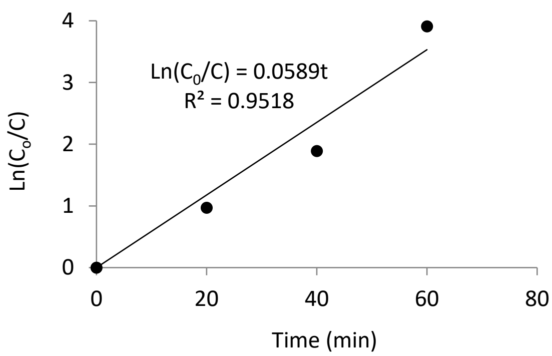

Fig. 5. First-order reaction kinetics for the decolorization of RR33 by O_3/UV process (dye concentration, 100 ppm, pH, 7.99, superficial gas velocity, 0.18 cm/s)

The advantages of ozone over other oxidants are as follows: the fact that the degradable products of ozonation are generally non-toxic; its final products are CO_2 and H_2O; and the residual O_3 in the system changes in a few minutes to O_2 [63]. A comparison between different oxidants was also carried out by Atchariyawuta et al. [64] and they found that O_3 generally produced nontoxic products which were finally converted to CO_2 and H_2O if the conditions were extreme enough. Finally, as an example, the products of a decolorization break-down resulting from a direct dye using ozonation were subjected to toxicity and biodegradability tests. It was found that the oxidation products were non-toxic to algae and had a high tendency for biodegradation [51].

4. Conclusions

Both RSM and ANN techniques were applied for the modeling of the degradation of a colored solution of Reactive Red 33 by the UV/O_3 process in a bubble column reactor. The effects of time, superficial gas velocity, initial concentration of dye, and pH on the decolorization efficiency of RR33 were investigated. The overall efficiency of the UV/O_3 process was enhanced by operating at a basic pH. The efficiency of the AOPs gradually decreased with an increase in the initial concentration of the dye. It can be seen that the decolorization yield increased with an increase in time and superficial gas velocity. The ANN model was found to be capable of better predicting the decolorization efficiency of RR33 within the range it trained than the RSM model. The results of the ANN model indicated that it was much more robust and accurate in estimating the values of dependent variables when compared with the RSM model.

References

[1] Essadki, A. H., Bennajah, M., Gourich, B., Vial, C., Azzi, M., Delmas, H. (2008). Electrocoagulation /electroflotation in an external-loop airlift reactor—application to the decolorization of textile dye wastewater: a case study. *Chemical engineering and processing: Process intensification*, *47*(8), 1211-1223.

[2] Daneshvar, N., Khataee, A. R., Ghadim, A. A., Rasoulifard, M. H. (2007). Decolorization of CI Acid Yellow 23 solution by electrocoagulation process: Investigation of operational parameters and evaluation of specific electrical energy consumption (SEEC). *Journal of hazardous materials*, *148*(3), 566-572.

[3] Wu, C. H., Chang, C. L. (2006). Decolorization of Reactive Red 2 by advanced oxidation processes: Comparative studies of homogeneous and heterogeneous systems. *Journal of hazardous materials*, *128*(2), 265-272.

[4] Anjaneyulu, Y., Chary, N. S., Raj, D. S. S. (2005). Decolourization of industrial effluents–available methods and emerging technologies–a review. *Reviews in environmental science and biotechnology*, *4*(4), 245-273.

[5] Saratale, R. G., Saratale, G. D., Chang, J. S., Govindwar, S. P. (2011). Bacterial decolorization and degradation of azo dyes: A review. *Journal of the Taiwan institute of chemical engineers*, *42*(1), 138-157.

[6] Wu, C. H., Kuo, C. Y., Chang, C. L. (2007). Decolorization of azo dyes using catalytic ozonation. *Reaction kinetics and catalysis letters*, *91*(1), 161-168.

[7] Golder, A. K., Hridaya, N., Samanta, A. N., Ray, S. (2005). Electrocoagulation of methylene blue and eosin yellowish using mild steel electrodes. *Journal of hazardous materials*, *127*(1), 134-140.

[8] Do, J. S., Chen, M. L. (1994). Decolourization of dye-containing solutions by electrocoagulation. *Journal of applied electrochemistry*, *24*(8), 785-790.

[9] Jiang, J. Q., Graham, N. J. D. (1996). Enhanced coagulation using Al/Fe (III) coagulants: effect of coagulant chemistry on the removal of colour-causing NOM. *Environmental technology*, *17*(9), 937-950.

[10] Slokar, Y. M., Le Marechal, A. M. (1998). Methods of decoloration of textile wastewaters. *Dyes and pigments*, *37*(4), 335-356.

[11] Li, G., Zhao, X. S., Ray, M. B. (2007). Advanced oxidation of orange II using TiO_2 supported on porous adsorbents: The role of pH, H_2O_2 and O_3. *Separation and purification technology*, *55*(1), 91-97.

[12] He, Z., Lin, L., Song, S., Xia, M., Xu, L., Ying, H., Chen, J. (2008). Mineralization of CI reactive blue 19 by ozonation combined with sonolysis: Performance optimization and degradation mechanism. *Separation and purification technology*, *62*(2), 376-381.

[13] Sanches, S., Crespo, M. T. B., Pereira, V. J. (2010). Drinking water treatment of priority pesticides using

low pressure UV photolysis and advanced oxidation processes. *Water research*, *44*(6), 1809-1818.

[14] Gogate, P. R., Pandit, A. B. (2004). A review of imperative technologies for wastewater treatment I: oxidation technologies at ambient conditions. *Advances in environmental research*, *8*(3), 501-551.

[15] Mohajerani, M., Mehrvar, M., Ein-Mozaffari, F. (2012). Using an external-loop airlift sonophotoreactor to enhance the biodegradability of aqueous sulfadiazine solution. *Separation and purification technology*, *90*, 173-181.

[16] Lucas, M. S., Peres, J. A., Puma, G. L. (2010). Treatment of winery wastewater by ozone-based advanced oxidation processes (O_3, O_3/UV and O_3/UV/H_2O_2) in a pilot-scale bubble column reactor and process economics. *Separation and purification technology*, *72*(3), 235-241.

[17] Beltran, F. J. (2003). *Ozone reaction kinetics for water and wastewater systems*. CRC Press.

[18] Khan, H., Ahmad, N., Yasar, A., Shahid, R. (2010). Advanced oxidative decolorization of Red Cl-5B: Effects of dye concentration, process optimization and reaction kinetics. *Polish journal of environmental studies.*, *19*(1), 83-92.

[19] Beltrán, F. J., Encinar, J., González, J. F. (1997). Industrial wastewater advanced oxidation. Part 2. Ozone combined with hydrogen peroxide or UV radiation. *Water research*, *31*(10), 2415-2428.

[20] Alnaizy, R., Akgerman, A. (2000). Advanced oxidation of phenolic compounds. *Advances in environmental research*, *4*(3), 233-244.

[21] Gimeno, O., Carbajo, M., Beltrán, F. J., Rivas, F. J. (2005). Phenol and substituted phenols AOPs remediation. *Journal of hazardous materials*, *119*(1), 99-108.

[22] Esplugas, S., Gimenez, J., Contreras, S., Pascual, E., Rodriguez, M. (2002). Comparison of different advanced oxidation processes for phenol degradation, *Water research*, 36(4), 1034-1042.

[23] Shu, H. Y., Chang, M. C. (2005). Decolorization effects of six azo dyes by O_3, UV/O_3 and UV/H_2O_2 processes. *Dyes and pigments*, *65*(1), 25-31.

[24] Peternel, I., Koprivanac, N., Kusic, H. (2006). UV-based processes for reactive azo dye mineralization. *Water research*, *40*(3), 525-532.

[25] Maran, J. P., Sivakumar, V., Sridhar, R., Immanuel, V. P. (2013). Development of model for mechanical properties of tapioca starch based edible films. *Industrial crops and products*, *42*, 159-168.

[26] Maran, J. P., Sivakumar, V., Sridhar, R., Thirugnanasambandham, K. (2013). Development of model for barrier and optical properties of tapioca starch based edible films. *Carbohydrate polymers*, *92*(2), 1335-1347.

[27] Maran, J. P., Manikandan, S., Nivetha, C. V., Dinesh, R. (2013). Ultrasound assisted extraction of bioactive compounds from Nephelium lappaceum L. fruit peel using central composite face centered response surface design. *Arabian journal of chemistry* http://dx.doi.org/10/1016/j.arabjc.2013.002.007

[28] Hemmat, J., MazaheriAssadi, M. (2013). Optimization of reactive blue 19 biodegradation by Phanerochaetechrysosporium. *International journal of environmental research*, *7*(4), 957-962.

[29] Berkani, M., Bouhelassa, M., Bouchareb, M. K. (2015). Implementation of a venturi photocatalytic reactor: Optimization of photodecolorization of an industrial azo dye. *Arabian Journal of Chemistry*, *http://dx.doi.org/10.1016/j.arabjc.2015.07.004.*

[30] Zobel, C. W., Cook, D. F. (2011). Evaluation of neural network variable influence measures for process control. *Engineering applications of artificial intelligence*, *24*(5), 803-812.

[31] Alavala, C. R. (2007). Logic and Neural Networks: Basic concepts and applications. *New Age. New Age Publications*.

[32] Pilkington, J. L., Preston, C., Gomes, R. L. (2014). Comparison of response surface methodology (RSM) and artificial neural networks (ANN) towards efficient extraction of artemisinin from Artemisia annua. *Industrial crops and products*, *58*, 15-24.

[33] Aber, S., Daneshvar, N., Soroureddin, S. M., Chabok, A., Asadpour-Zeynali, K. (2007). Study of acid orange 7 removal from aqueous solutions by powdered activated carbon and modeling of experimental results by artificial neural network. *Desalination*, *211*(1), 87-95.

[34] Zarei, M., Khataee, A. R., Ordikhani-Seyedlar, R., Fathinia, M. (2010). Photoelectro-Fenton combined with photocatalytic process for degradation of an azo dye using supported TiO_2 nanoparticles and carbon nanotube cathode: neural network modeling. *Electrochimica Acta*, *55*(24), 7259-7265.

[35] Zarei, M., Niaei, A., Salari, D., Khataee, A. R. (2010). Removal of four dyes from aqueous medium by the peroxi-coagulation method using carbon nanotube–PTFE cathode and neural network modeling. *Journal of electroanalytical chemistry*, *639*(1), 167-174.

[36] Cheok, C. Y., Chin, N. L., Yusof, Y. A., Talib, R. A., Law, C. L. (2012). Optimization of total phenolic content extracted from Garcinia mangostana Linn. Hull using response surface methodology versus artificial neural network. *Industrial crops and products*, *40*, 247-253.

[37] Khajeh, M., Kaykhaii, M., Sharafi, A. (2013). Application of PSO-artificial neural network and response surface methodology for removal of methylene blue using silver nanoparticles from water samples. *Journal of industrial and engineering chemistry*, *19*(5), 1624-1630.

[38] Ebrahimzadeh, H., Tavassoli, N., Sadeghi, O., Amini, M. M. (2012). Optimization of solid-phase extraction using artificial neural networks and response surface methodology in combination with experimental design for determination of gold by atomic absorption spectrometry in industrial wastewater samples. *Talanta*, *97*, 211-217.

[39] Khayet, M., Cojocaru, C. (2013). Artificial neural network model for desalination by sweeping gas membrane distillation. *Desalination*, *308*, 102-110.

[40] Lakshminarayanan, A. K., Balasubramanian, V. (2009). Comparison of RSM with ANN in predicting tensile strength of friction stir welded AA7039 aluminium alloy joints. *Transactions of nonferrous metals society of China*, *19*(1), 9-18.

[41] Sinha, K., Saha, P. D., Datta, S. (2012). Response surface optimization and artificial neural network modeling of microwave assisted natural dye extraction from pomegranate rind. *Industrial crops and products*, *37*(1), 408-414.

[42] Maran, J. P., Sivakumar, V., Thirugnanasambandham, K., Sridhar, R. (2013). Artificial neural network and response surface methodology modeling in mass transfer parameters predictions during osmotic dehydration of Carica papaya L. *Alexandria engineering journal*, *52*(3), 507-516.

[43] Yang, S. H., Chung, P. W. H., Brooks, B. W. (1999). Multi-stage modelling of a semi-batch polymerization reactor using artificial neural networks. *Chemical engineering research and design*, *77*(8), 779-783.

[44] Bassam, A., Ortega-Toledo, D., Hernandez, J. A., Gonzalez-Rodriguez, J. G., Uruchurtu, J. (2009). Artificial neural network for the evaluation of CO2 corrosion in a pipeline steel. *Journal of solid state electrochemistry*, *13*(5), 773-780.

[45] Baughman, D. R., Liu, Y. A. (2014). *Neural networks in bioprocessing and chemical engineering*. Academic press.

[46] Kusic, H., Koprivanac, N., Bozic, A. L. (2006). Minimization of organic pollutant content in aqueous solution by means of AOPs: UV-and ozone-based technologies. *Chemical engineering journal*, *123*(3), 127-137.

[47] Peternel, I., Koprivanac, N., Kusic, H. (2006). UV-based processes for reactive azo dye mineralization. *Water research*, *40*(3), 525-532.

[48] Sevimli, M. F., Sarikaya, H. Z. (2002). Ozone treatment of textile effluents and dyes: effect of applied ozone dose, pH and dye concentration. *Journal of chemical technology and biotechnology*, *77*(7), 842-850.

[49] Azbar, N., Yonar, T., Kestioglu, K. (2004). Comparison of various advanced oxidation processes and chemical treatment methods for COD and color removal from a polyester and acetate fiber dyeing effluent. *Chemosphere*, *55*(1), 35-43.

[50] Sevimli, M. F., Sarikaya, H. Z. (2005). Effect of some operational parameters on the decolorization of textile effluents and dye solutions by ozonation. *Environmental technology*, *26*(2), 135-144.

[51] Konsowa, A. H. (2003). Decolorization of wastewater containing direct dye by ozonation in a batch bubble column reactor. *Desalination*, *158*(1), 233-240.

[52] Selcuk, H. (2005). Decolorization and detoxification of textile wastewater by ozonation and coagulation processes. *Dyes and pigments*, *64*(3), 217-222.

[53] Aksu, Z. (2003). Reactive dye bioaccumulation by Saccharomyces cerevisiae. *Process biochemistry*, *38*(10), 1437-1444.

[54] Asad, S., Amoozegar, M. A., Pourbabaee, A., Sarbolouki, M. N., Dastgheib, S. M. M. (2007). Decolorization of textile azo dyes by newly isolated halophilic and halotolerant bacteria. *Bioresource technology*, *98*(11), 2082-2088.

[55] Wu, J., Wang, T. (2001). Ozonation of aqueous azo dye in a semi-batch reactor. *Water research*, *35*(4), 1093-1099.

[56] Wang, K. H., Hsieh, Y. H., Wu, C. H., Chang, C. Y. (2000). The pH and anion effects on the heterogeneous photocatalytic degradation of o-methylbenzoic acid in TiO_2 aqueous suspension. *Chemosphere*, *40*(4), 389-394.

[57] Zhang, H., Duan, L., Zhang, D. (2006). Decolorization of methyl orange by ozonation in combination with ultrasonic irradiation. *Journal of hazardous materials*, *138*(1), 53-59.

[58] Yetilmezsoy, K., Demirel, S. (2008). Artificial neural network (ANN) approach for modeling of Pb (II) adsorption from aqueous solution by Antep pistachio (Pistacia Vera L.) shells. *Journal of hazardous materials*, *153*(3), 1288-1300.

[59] Bingöl, D., Hercan, M., Elevli, S., Kılıç, E. (2012). Comparison of the results of response surface methodology and artificial neural network for the biosorption of lead using black cumin. *Bioresource technology*, *112*, 111-115.

[60] Bali, U., Çatalkaya, E., Şengül, F. (2004). Photodegradation of reactive black 5, direct red 28 and direct yellow 12 using UV, UV/H_2O_2 and $UV/H_2O_2/Fe^{2+}$: a comparative study. *Journal of hazardous materials*, *114*(1), 159-166.

[61] Wu, J., Wang, T. (2001). Ozonation of aqueous azo dye in a semi-batch reactor. *Water research*, *35*(4), 1093-1099.

[62] Neamtu, M., Yediler, A., Siminiceanu, I., Kettrup, A. (2003). Oxidation of commercial reactive azo dye aqueous solutions by the photo-Fenton and Fenton-like processes. *Journal of photochemistry and photobiology A: Chemistry*, *161*(1), 87-93.

[63] Guendy, H. R. (2007). Ozone treatment of textile wastewater relevant to toxic effect elimination in

marine environment. *Egyptian journal of aquatic research*, 33 (1), 98-115.

[64] Atchariyawut, S., Phattaranawik, J., Leiknes, T., Jiraratananon, R. (2009). Application of ozonation membrane contacting system for dye wastewater treatment. *Separation and purification technology*, *66*(1), 153-158.